JOURNAL OF THEORETICAL AND APPLIED MECHANICS
51, 2, pp. 475-486, Warsaw 2013

ANALYSIS OF THE PRIMARY AND SUPERHARMONIC CONTACT RESONANCES – PART 1

Robert Kostek
University of Technology and Life Sciences in Bydgoszcz, Poland
e-mail: robertkostek@o2.pl

This paper presents results of numerical and analytical investigations of non-linear normal contact microvibrations excited by a harmonic force in a system of two bodies in planar contact. The system models, for example, the slide unit of machine tools or positioning systems. The main aim of the computational analysis is to present the evolution of the resonance phenomena under various amplitudes of the excitation force. The studies show that, beside the primary resonance, a number of superharmonic resonances appear, which take place in the single-degree-of-freedom non-linear system excited by a harmonic force. Thus, in a resonance plot, a number of peaks is observed. The superharmonic (ultraharmonic) resonances take place at excitation frequencies being below the natural frequency, and becoming stronger with the increase of the excitation amplitude. The resonances are coupled with complex non-linear phenomena like: asymmetry of vibrations, bending resonance peak, bi-stability, multi-stability and loss of contact, which are presented and described in this paper.

Key words: non-linear contact, vibrations, superharmonic resonance, multi-stability

1. Introduction

In the modelling of mechanical systems, the essential fact that the contact of rough surfaces is flexible and strongly non-linear should not be neglected. The contact phenomena are likely to affect the behaviour of machines (Fan *et al.*, 2012; Shi and Polycarpou, 2005; Thomas, 1999). For instance, contact flexibility has influence on the static stiffness of machine tools, where contact deflections can be larger than distortions of machine parts (Chlebus and Dybala, 1999; Gutowski, 2003; Kaminskaya *et al.*, 1960; Levina and Reshetov, 1971; Marchelek, 1974); thus most parts of the machines can be modelled as rigid bodies (Gutowski, 2003; Marchelek, 1974). The phenomena refer, in particular, to precision machines, such as grinding machines. Thus, in turn, the contact flexibility affects dynamic properties of machines and, consequently, their precision, productivity, stability and vibrations (e.g. chatter) (Dhupia *et al.*, 2007; Fan *et al.*, 2012; Gutowski, 2003; Huo *et al.*, 2010; Marchelek, 1974; Moradi *et al.*, 2010; Neugebauer *et al.*, 2007). It is known that frequencies of the excitation force (cutting force) should be out of the resonance area, in order to reduce amplitude of vibrations and make machining stable (Gutowski, 2003; Marchelek, 1974). These are the reasons why the contact phenomena (deflection, vibration, friction, damping and wear) have currently become one of the main areas of scientific activity.

The resonance is one of the most important and common issue in dynamics, thus a number of articles has been written on contact resonances. Most of them are focused only on the primary contact resonance (Chajkin *et al.*, 1939; Grigorova and Tolstoi, 1966; Hess and Soom, 1991a,b; Kligerman, 2003; Rigaud and Perret-Liaudet, 2003; Tolstoi, 1967), while still a few are on the superharmonic resonances (Grudziński and Kostek, 2007; Kostek, 2004; Perret-Liaudet, 1998; Perret-Liaudet and Rigad, 2007). Most of the papers present vibrations excited within a narrow range of frequencies and amplitudes, hence there is a need to present an analysis of the contact vibrations excited with a wide range of frequencies and amplitudes of the excitation force.

The present study is focused on the evolution of primary and superharmonic resonances due to various amplitudes of the excitation. The superharmonic resonances can amplify the amplitude of vibrations being excited with an excitation frequency which is below the natural frequency. In machine tools, the resonances can affect chatter (Moradi *et al.*, 2010). The problems have been found important in the context of the dynamics of precise machine tools where low amplitudes of vibrations are required.

2. Theoretical fundamentals

The considered system consists of two bodies in planar contact (Fig. 1), which is modelled in this section. The system can be viewed as a simplified model of a slide unit of a machine tool. The system consists of a rigid block (slider) resting on a massive rigid base (slideway). The interface of the bodies, which represents the planar contact of rough surfaces, is modelled with a great number of microsprings and microdampers (Fig. 1b). The microsprings and microdampers represent the interacting roughness of asperities. It has been assumed that the spring–damping properties of the interface are macroscopically identical over all the contact area. Thus, after homogenisation (Fig. 1c), the contact zone is modelled with one non-linear spring and damper (Figs. 1d,e).

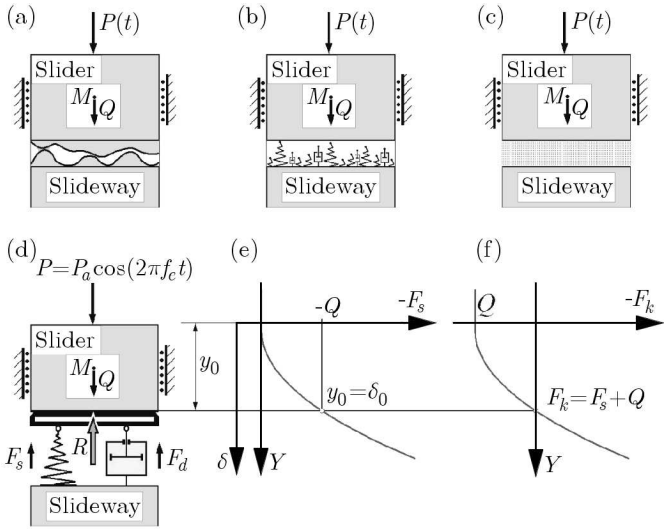

Fig. 1. Scheme of the considered dynamical system (a), and its physical models (b)-(d), characteristic of the spring force F_s (e), characteristic of the conservative force F_k (f)

The displacement of the vibrating body (slider) y is determined by the coordinate Y with respect to the rigid base (slideway). The coordinate system is pointing downward (Fig. 1e), and the origin is fixed on the level where the contact deflection δ begins; therefore, $y = 0$ implies $\delta = 0$. Thus the contact deflection $\delta = y$, if $y > 0$, and $\delta = 0$, if $y \leqslant 0$. This convention allows for simulation of "gapping" (loss of contact) in the case of large contact vibrations. A very important parameter is the static contact deflection due to the weight of the slider $\delta_0 = y_0$, which determines the equilibrium position.

The contact force (reaction) R is the sum of the spring force Fs and the damping force F_d (Fig. 1d). The spring force is a non-linear function of the displacemen y, whereas the damping force is a non-linear function of the displacement y and velocity $\dot{y}$. The forces are described by the following formulas (Hunt and Crossley, 1975; Kostek, 2004; Martins *et al.*, 1990)

$$\begin{aligned} &\text{IF} \quad y > 0 \quad \text{THEN} \quad F_s = -Sc_n y^{m_2}\,, \quad F_d = -Sh_n y^l \dot{y}\,, \quad \delta = y \\ &\text{ELSE} \quad F_s = 0\,, \quad F_d = 0\,, \quad \delta = 0 \end{aligned} \tag{2.1}$$

where S denotes the nominal (apparent) contact area, while c_n, m_2, h_n, and l are parameters of the contact interface, and δ is the normal contact deflection. Values of the parameters have been identified from experimental results (Grudziński *et al.*, 2000; Grudziński and Kostek, 2007; Kostek, 2002, 2004); thus reliable values of the parameters have been adopted to the simulations: $S = 0.0009\,\mathrm{m}^2$, $c_n = 4.52693 \cdot 10^{16}\,\mathrm{N/m}^4$, $m_2 = 2$, $h_n = 3.5 \cdot 10^{11}\,\mathrm{Ns/m}^4$, $l = 1$. Moreover, the adopted model of contact was validated against the experimental results (Hess and Soom, 1992; Hess and Wagh, 1995; Kostek, 2004). For further information please see appendix.

Apart from the spring and the damping contact forces, two more forces act on the slider (Fig. 1). They are: the exciting (driving) harmonic force P, and the terrestrial gravity force Q, which are expressed by the following formulas

$$P = P_a \cos(2\pi f_e t) \qquad Q = Mg \tag{2.2}$$

where P_a denotes the amplitude of the exciting force, f_e – frequency of excitation, t – time, M – mass of the slider $M = 0.2106\,\mathrm{kg}$, and g – acceleration of gravity $g = 9.81\,\mathrm{m/s}^2$. The magnitude of mass is adopted for a cube made of steel, whose width, length and height are 30 mm.

The sum of the spring force F_s and the terrestrial gravity force Q can be treated as the conservative force

$$F_k = F_s + Q \tag{2.3}$$

The conservative force F_k is a source of non-linearity in the system. The graph of the conservative force F_k is asymmetrical (Fig. 1f). Therefore, different values of the force are observed for the same displacement magnitude, depending on whether the displacement is up or down from the equilibrium position. Finally, the contact vibrations of the adopted model (Fig. 1d) are described by the following equation

$$\ddot{y} = M^{-1}(F_k(y) + F_d(y, \dot{y}) + P(t)) \tag{2.4}$$

The formulated differential equation of motion is non-linear, because of the non-linearity of the spring and the damping contact forces. The equation can be solved numerically using the 4-th order Runge-Kutta method, which was used to obtain the resonant characteristics of the system. The system was excited by a constant amplitude harmonic force. After the steady-state response was attained, local minima and maxima of the time history were noted. Finally, the frequency of excitation f_e was changed. The procedure allows for simulation of complex resonance phenomena (Figs. 2 and 3), which are presented in the next sections.

Apart from the numerical methods, the contact microvibrations can be studied with perturbation methods. In this case, the conservative force F_k can be described by the Taylor series, around the equilibrium position, while the damping force F_d can be linearised around the equilibrium position, which leads to the following equations

$$\begin{aligned} F_k &= Mg - Sc_n y_0^{m_2} - Sc_n m_2 y_0^{m_2-1}(y - y_0) \\ &\quad - \frac{1}{2} Sc_n m_2 (m_2 - 1) y_0^{m_2-2}(y - y_0)^2 + O(y - y_0)^3 \\ F_d &= -Sh_n y_0^l \dot{y} \end{aligned} \tag{2.5}$$

Finally, after dividing the equation of motion by M, the vibrations are described by the following formulas

$$\ddot{u} + 2c\dot{u} + \omega_0^2 u + \varepsilon h u^2 = G\cos(2\pi f_e t) \qquad u = y - y_0 \tag{2.6}$$

where u denotes displacement, while

$$2c = M^{-1}Sh_n y_0^l \qquad \omega_0^2 = M^{-1}Sc_n m_2 y_0^{m_2-1}$$
$$\varepsilon h = \frac{1}{2}M^{-1}Sc_n m_2(m_2-1)y_0^{m_2-2} \qquad G = M^{-1}P_a$$

are parameters of the equation, and ε is the small parameter associated with the non-linear term. The solution is formed in terms of an infinite series of the perturbation parameter as follows (Awrejcewicz, 1996; Nayfeh and Mook, 1995)

$$\begin{aligned}\omega^2 &= \omega_0^2 + \varepsilon b_1 + \varepsilon^2 b_2 + \ldots \\ u &= u_0(t) + \varepsilon u_1(t) + \varepsilon^2 u_2(t) + \ldots\end{aligned} \tag{2.7}$$

where ω_0 denotes natural frequency of the undamped linearised system, ω natural frequency of the non-linear system, while b_1, b_2, ... are functions of amplitudes, and $u_0(t)$, $u_1(t)$, $u_2(t)$, ... are terms of the solution. Submitting Eqs. (2.7) into Eq. $(2.6)_1$ leads to a system of linear equations, which can be solved successively:

— ε^0

$$\ddot{u}_0 + 2c\dot{u}_0 + \omega^2 u_0 = G\cos(2\pi f_e t) \qquad u_0 = A_0\cos(2\pi f_e t + \varphi_0) \tag{2.8}$$

— ε^1

$$\begin{aligned}&\ddot{u}_1 + 2c\dot{u}_1 + \omega^2 u_1 = b_1 u_0 - h u_0^2 = b_1 A_0\cos(2\pi f_e t + \varphi_0) - hA_0^2\cos^2(2\pi f_e t + \varphi_0) \\ &\quad = b_1 A_0\cos(2\pi f_e t + \varphi_0) - \frac{1}{2}hA_0^2\cos(4\pi f_e t + 2\varphi_0) - \frac{1}{2}hA_0^2 \\ &b_1 = 0 \\ &u_1 = A_1\cos(4\pi f_e t + 2\varphi_0 + \varphi_1) + A_2\end{aligned} \tag{2.9}$$

— ε^2

$$\begin{aligned}&\ddot{u}_2 + 2c\dot{u}_2 + \omega^2 u_2 = b_1 u_1 + b_2 u_0 - 2h u_0 u_1 = b_2 A_0\cos(2\pi f_e t + \varphi_0) \\ &\quad - 2hA_0\cos(2\pi f_e t + \varphi_0)[A_1\cos(4\pi f_e t + 2\varphi_0 + \varphi_1) + A_2] \\ &\quad = b_2 A_0\cos(2\pi f_e t + \varphi_0) - 2hA_0 A_2\cos(2\pi f_e t + \varphi_0) \\ &\quad - hA_0 A_1\cos(2\pi f_e t + \varphi_0 + \varphi_1) - hA_0 A_1\cos(6\pi f_e t + 3\varphi_0 + \varphi_1) \\ &b_2 = 2hA_2 + hA_1\cos\varphi_1 \\ &u_2 = A_3\cos(2\pi f_e t + 2\varphi_0) + A_4\cos(2\pi f_e t + 2\varphi_0) + A_5\cos(2\pi f_e t + 2\varphi_0 + \varphi_1) \\ &\quad + A_6\cos(6\pi f_e t + 3\varphi_0 + \varphi_1 + \varphi_2) = A_7\cos(2\pi f_e t + 2\varphi_0) \\ &\quad + A_5\cos(2\pi f_e t + 2\varphi_0 + \varphi_1) + A_6\cos(6\pi f_e t + 3\varphi_0 + \varphi_1 + \varphi_2)\end{aligned} \tag{2.10}$$

where A_0-A_7 are amplitudes and φ_0-φ_2 are phase angles. Similar non-linear vibrations have been previously studied with the perturbation method (Hess and Soom, 1991a,b; Nayak, 1972; Nayfeh, 1983; Nayfeh and Mook, 1995; Perret-Liaudet, 1998; Perret-Liaudet and Rigad, 2007) that shows the complexity of the issue. The obtained approximate solution to the Eq. $(2.6)_1$ is interpreted in the next section, while Appendix contains more information and equations.

3. The contact resonances

The normal contact vibrations, which are common in machine tools, are coupled with oscillations of the slider about the equilibrium position $y_0 = \delta_0$. When the amplitude of the contact vibrations is very small, then the vibrations are linear and the natural frequency of the considered system equals $f_{n0} = 1485\,\text{Hz}$. The perturbation solution reflects the phenomena, because the terms hA_0^2, hA_0A_1, u_1, u_2 and b_2 are close to zero in this case (Eqs. (2.9) and (2.10)). In linear systems, the number of resonance peaks is not larger than the number of degrees-of-freedom.

Thus, no more than one resonance peak is found, for a single degree-of-freedom linear system. In contrast, many kinds of resonances may be found in a non-linear single degree-of-freedom system (Awrejcewicz, 1996; Belhaq and Fahsi, 2009; Bogusz *et al.*, 1974; Cunningham, 1958; Fyrillas and Szeri, 1998; Nayfeh and Mook, 1995; Parlitz and Lauterborn, 1985; Tang, 2000; Thompson and Stewart, 2002). Therefore, many peaks can appear in a resonance graph (Fyrillas and Szeri, 1998; Grudziński and Kostek, 2007; Kostek, 2004; Nayfeh and Mook, 1995; Parlitz and Lauterborn, 1985; Thompson and Stewart, 2002). The resonances can take place when the exciting frequency f_e is in the following relation to the natural frequency f_{n0}

$$f_e \approx \frac{n}{m} f_{n0} \tag{3.1}$$

where m and n are positive integers. Depending on the values of these integers, the following kinds of resonances may take place in the system (Awrejcewicz, 1996; Bogusz *et al.*, 1974; Nayfeh and Mook, 1995):

- primary (main) resonance, if $n = 1$, $m = 1$,
- superharmonic (ultraharmonic) resonance, if $n = 1$, $m > 1$,
- subharmonic resonance, if $n > 1$, $m = 1$, and
- super-subharmonic resonance, if $m \neq 1$, $n \neq 1$ and $n/m \neq 1$.

The contact resonances can be presented graphically in different ways. They can be shown as a peak-to-peak amplitude $A_{pp} = y_{max} - y_{min}$ in the logarithmic scale against the frequency of excitation f_e. This allows the presentation of a wide range of amplitudes, and the figure is easy to interpret (Fig. 2). More information can be provided if all local extrema in the time response (over one period of vibration) are presented as a function of the excitation frequency f_e (Fig. 3). This figure presents the following: a complex structure of the superharmonic resonances, the asymmetry of contact vibrations, and "gapping". If the slider loses contact with the slideway, then the minima reach negative values. The appearance of more than two extrema per period leads to more than two curves in the resonance graph. The issues are described in the next paper. Generally, the way of presentation of the resonances should be fitted to the aim of the presentation.

3.1. The primary resonance

In the case of a very small amplitude of the excitation force P_a, the simulated vibrations are linear and the resonance is linear (Kostek, 2004), and the nature of the primary resonance is clear. The loss of energy caused by the damping force F_d is compensated with the work done by the external harmonic force P. The process is particularly effective when the frequency of excitation f_e is near the natural frequency f_{n0}. Therefore, the amplitude of the vibrations is the largest near the natural frequency f_{n0}.

Gradually, with the increase of the excitation amplitude P_a, the contact vibrations become larger and non-linear. Thus, the phenomena typical for non-linear vibrations take place (Grudziński and Kostek, 2007; Kostek, 2004). The non-linear conservative force F_k, the graph of which is asymmetrical (Fig. 1f), introduces characteristic phenomena. The contact microvibrations become asymmetrical to the equilibrium position (Fig. 3) (see A_2 Eq. $(2.9)_3$), and finally, the slider can lose contact with the slideway (Figs. 3b-3j). If the slider loses contact with the slideway, then a minimum of the time history y_{min} attains a negative value (Eq. $(2.1)_1$), which reflects Fig. 3b-3j (see light gray curves). In other words, negative values of minima reveal the loss of contact. The natural frequency of the non-linear system is a function of the vibration amplitude (see Eqs. $(2.7)_1$ and $(2.10)_2$), and this, significantly, has influence on the resonance graph because the resonance peaks follow the natural frequency. In this case, they bend to

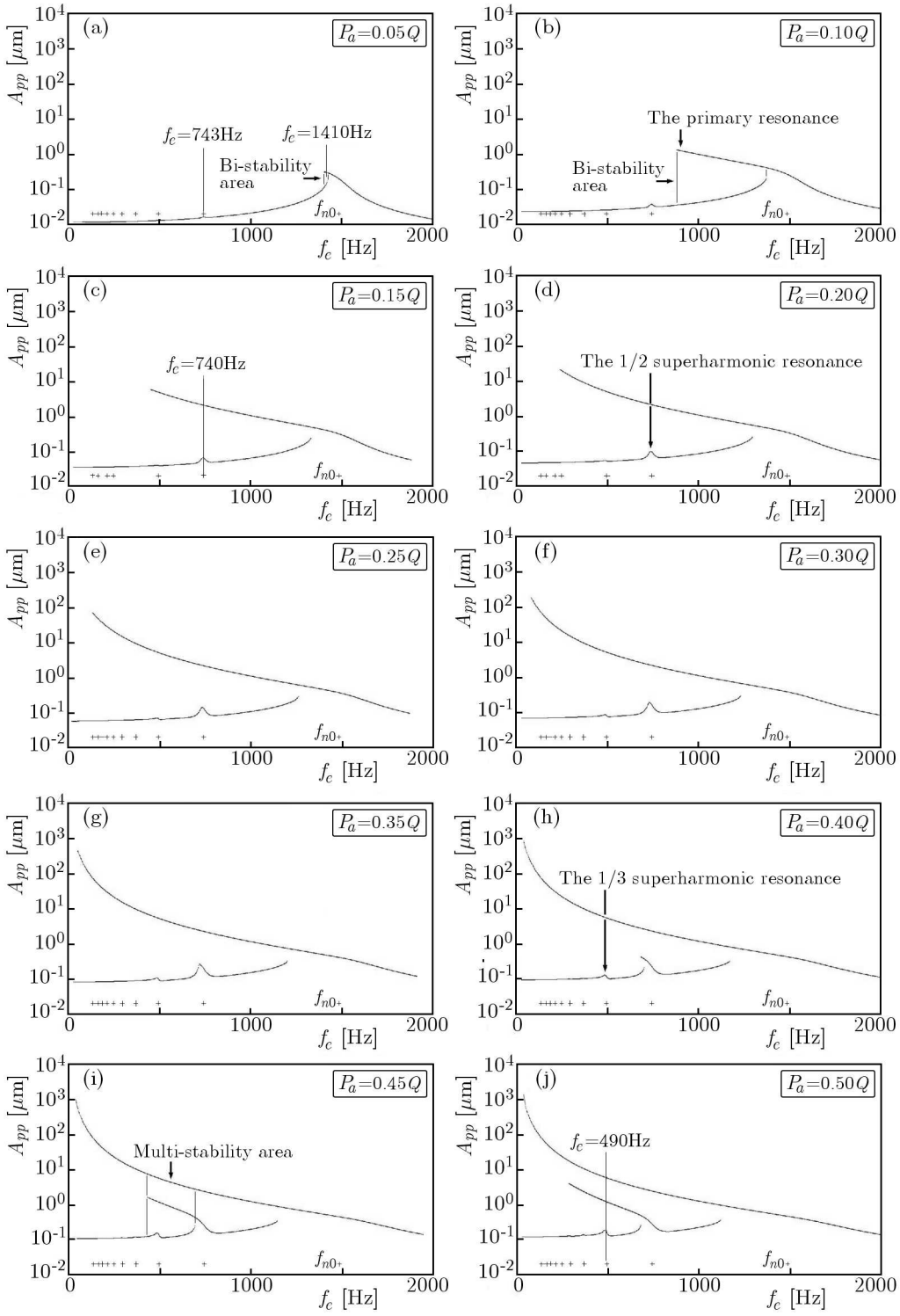

Fig. 2. Graphs of the contact resonances; peak-to-peak amplitude $A_{pp} = y_{max} - y_{min}$ against the frequency of excitation f_e; plus signs (+) represent resonant frequencies $f_e \approx f_{n0}/m$, Eq. (3.1)

the lower frequencies (Figs. 2 and 3), because the natural frequency becomes smaller with the increase of the vibration amplitude (see Eq. $(2.10)_2$). The bending of the primary resonance peak introduces bi-stability to the system; thus a response of the system is ambiguous at some frequencies of excitation f_e (Fig. 2c). Consequently, the obtained solution depends on initial conditions.

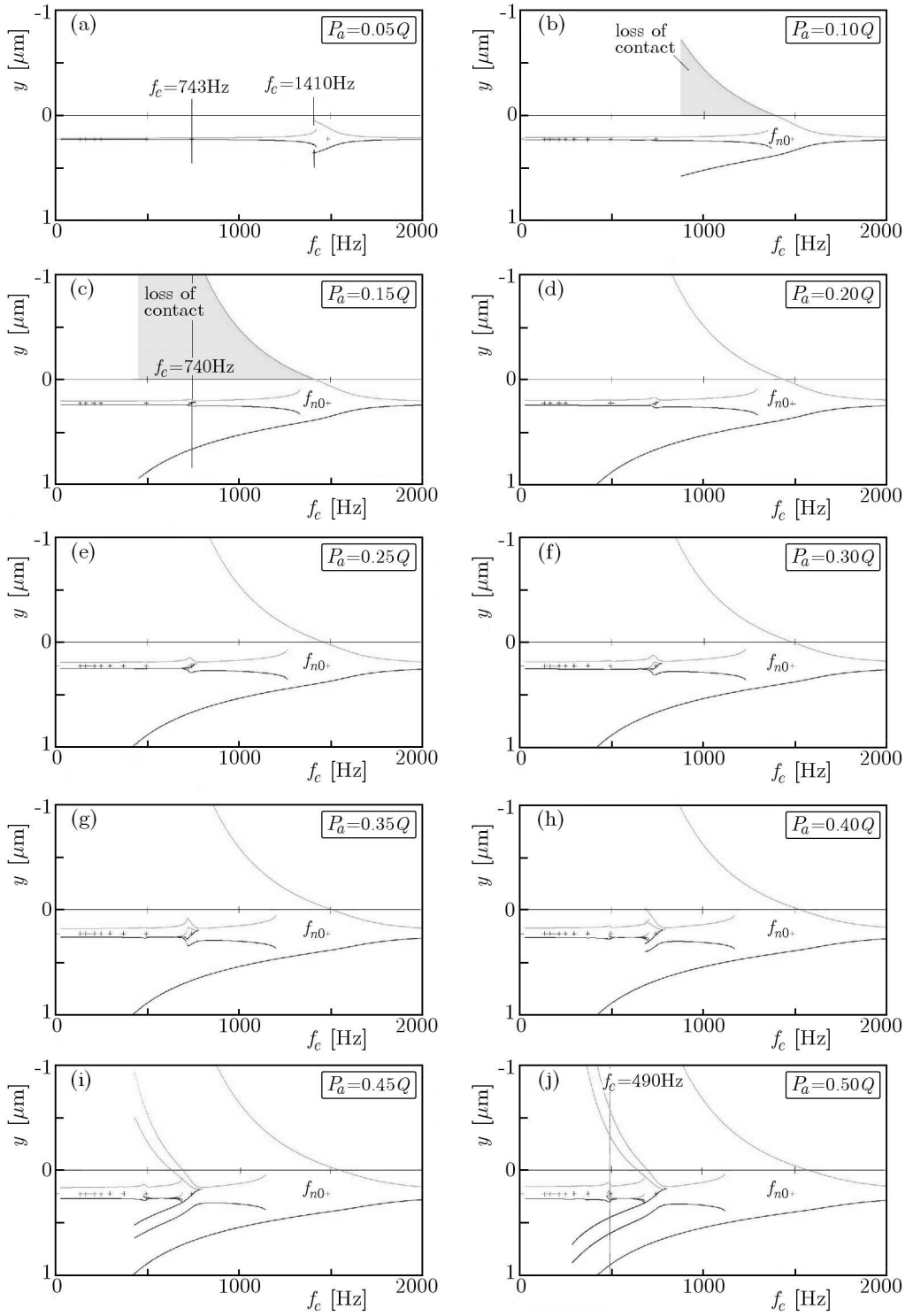

Fig. 3. Graphs of the contact resonances; local extrema of time histories against the frequency of excitation f_e; (light gray line – minima, dark gray line – maxima obtained with the numerical method)

3.2. The superharmonic resonances

Usually, analyses of dynamical systems are focused on the primary resonance, while the rest of the excitations are treated as safe. Nevertheless, apart from the primary resonance, a number of superharmonic resonances can take place, for frequencies of excitation being below the natural

frequency $f_e < f_{n0}$. Consequently, non-linear systems should be tested under a wide range of excitations, and the resonance phenomena should be studied as a whole.

Vibrations of the non-linear system excited by a harmonic force are multiharmonic (see Eqs. $(2.9)_3$ and $(2.10)_3$); thus they contain a number of harmonics. When the frequency of the m-th harmonic of the vibrations approaches the natural frequency, then the amplitude of the m-th harmonic is rising (see Eqs. $(2.9)_1$ and $(2.10)_1$). Thus, the frequencies of the superharmonic resonances form the series $f_e \approx (1/m) f_{n0}$. In other words, if the frequency of the 2-nd harmonic is near the natural frequency f_{n0}, then the frequency of excitation f_e is near the half of the natural frequency, $f_e \approx (1/2) f_{n0}$. As a result, the amplitude of the 2-nd harmonic is amplified (see Eq. $(2.9)_1$), and the $1/2$ superharmonic resonance is at this place (Fig. 2d). The next $1/3$ superharmonic resonance is a result of the amplification of the 3rd harmonic (see Eq. $(2.10)_1$), the frequency of which is near the natural frequency f_{n0}, $f_e \approx (1/3) f_{n0}$ (Fig. 2i), which, in turn, reflects the afore-mentioned relation Eq. (3.1). Summarising these, the nature of the superharmonic resonances is the amplification of higher harmonics, the frequency of which is near the natural frequency f_{n0}.

The phenomena such as asymmetry of vibrations, "gapping", and bending of the resonance peaks, take place at the superharmonic resonances too (Figs. 2 and 3). However, the resonances are far more complex than the primary resonance; that is, the nature of the superharmonic resonances. For instance, the magnification of higher harmonics makes time histories of the displacement, velocity and acceleration more complex, and a number of local minima and maxima is observed during one period of vibration. Consequently, more than two curves can represent super harmonic resonances, which affect the resonance graphs (Figs. 3c-3j). Finally, phase portraits, and spectrums, are more sophisticated as well. The spectrums, phase portraits, and time histories to be presented in the next paper clearly show the complexity of superharmonic resonances and their sophisticated kinematics.

3.3. The bi-stability and multi-stability

The primary resonance is non-linear. Its peak bends to lower frequencies (Figs. 2 and 3), thus a bi-stability area appears for $P_a = 0.05Q$ (Figs. 2a and 3a). The area of bi-stability becomes larger with a further increase of the excitation amplitude P_a. Therefore, for the excitation amplitude being $P_a = 0.15Q$, the primary resonance and the $1/2$ superharmonic resonance can be excited at the same frequency $f_e = 740\,\mathrm{Hz}$ (Figs. 2c and 3c). Next, the $1/2$ superharmonic resonance grows with the increase of the excitation amplitude. The further increase of the excitation amplitude leads to bending of the $1/2$ superharmonic resonance peak, which in turn introduces multi-stability to the system. In this case, three solutions are possible: the three resonances are excited, viz. the primary rezonance, the $1/2$ and $1/3$ superharmonic resonances for $P_a = 0.50Q$ and $f_e = 490\,\mathrm{Hz}$ (Figs. 2j and 3j). The visualization of the contact resonances is available on the Internet https://www.youtube.com/watch?v=cNRU-TUXCao.

4. Conclusions

The presented study has been focused on the evolution of contact resonances simulated for a wide range of excitations. The studied phenomena have been found to be important in the context of precision machining.

The contact vibrations are non-linear, thus a number of characteristic phenomena takes place. The vibrations are asymmetrical, thus a notion of the amplitude should be precisely defined, e.g. as the peak-to-peak amplitude A_{pp}. Furthermore, the natural frequency of the vibrations should be treated as a function of the vibration amplitude. Moreover, the resonances which take place in non-linear systems are far more complex than in linear ones. Apart from the primary resonance, a

number of superharmonic resonances takes place for frequencies of the excitation f_e being below the natural frequency f_{n0}. Their kinematics is complex, which is a result of the magnification of higher harmonics. The contact resonances become less intensive and more complex, with an increase of the integer m. An increase of the excitation amplitude P_a leads to an increase of their amplitudes, bending of the resonance peaks, and consequently, to bi-stability and finally multi-stability. Summarising these, a number of resonances and other non-linear phenomena influence the dynamics of the considered system. This shows that the contact vibrations and resonances should be studied under a wide range of excitation signals.

Simplified linear models of contact rough surfaces, which are typically used to model machine tool dynamics, do not allow the proper modelling of complex dynamical phenomena, e.g. chatter. Thus, to analyse these phenomena, non-linear models of contact, together with the theory of non-linear dynamics, should be used.

A. Appendix

Natural frequencies calculated for various heights of bodies h_b were compared with the experimental results published by Hess and Soom (1992), Hess and Wagh (1995). In spite of the fact that various contacts were tested, natural frequencies are similar (Fig. 4) (Kostek, 2002). Finally, the results of simulation obtained for the adopted model can be compared against the experimental results (Fig. 5). According with the presented results, one may conclude that reliable values of the parameters have been adapted to the simulations.

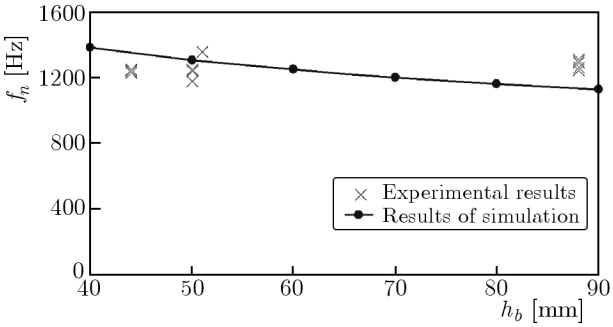

Fig. 4. Comparison of magnitudes of the natural frequencies f_n obtained experimentally for various heights of bodies h_b made of steel (Hess and Soom, 1992; Hess and Wagh, 1995) with results of simulation obtained for the rigid body and the adopted model of contact (Kostek, 2002)

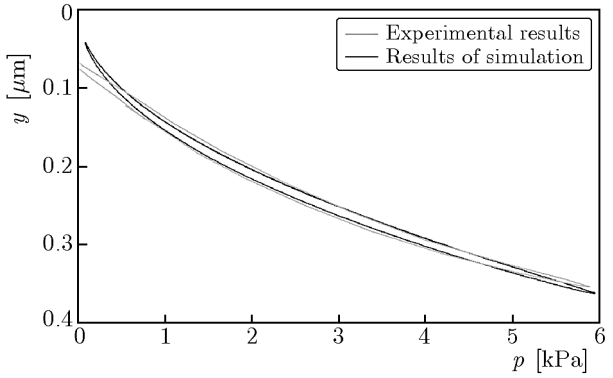

Fig. 5. Comparison of the hysteresis loop of contact obtained experimentally (Kostek, 2004) against the results of simulation carried out for $f_e = 1600\,\mathrm{Hz}$ and $P_a = 0.40Q$; displacement y versus normal contact pressure p

Further equations which are a part of the perturbation solution are presented below:

— ε^3

$$\begin{aligned}
&\ddot{u}_3 + 2c\dot{u}_3 + \omega^2 u_3 = b_1 u_2 + b_2 u_1 + b_3 u_0 - 2h u_0 u_2 - h u_1^2 \\
&\quad = b_2 A_1 \cos(4\pi f_e t + 2\varphi_0 + \varphi_1) + b_2 A_2 + b_3 A_0 \cos(2\pi f_e t + \varphi_0) \\
&\quad - h A_0 A_7 \cos(4\pi f_e t + 3\varphi_0) - h A_0 A_7 \cos(\varphi_0) - h A_0 A_5 \cos(4\pi f_e t + 3\varphi_0 + \varphi_1) \\
&\quad - h A_0 A_5 \cos(\varphi_0 + \varphi_1) - h A_0 A_6 \cos(8\pi f_e t + 4\varphi_0 + \varphi_1 + \varphi_2) \\
&\quad - h A_0 A_6 \cos(4\pi f_e t + 2\varphi_0 + \varphi_1 + \varphi_2) - \frac{1}{2} h A_1^2 \cos(8\pi f_e t + 4\varphi_0 + 2\varphi_1) \\
&\quad - \frac{1}{2} h A_1^2 - 2h A_1 A_2 \cos(4\pi f_e t + 2\varphi_0 + \varphi_1) - h A_2^2 \\
&\quad = A_8 + A_9 \cos(4\pi f_e t + \varphi_3) + A_{10} \cos(8\pi f_e t + \varphi_4) \\
&b_3 = 0 \\
&u_3 = A_{11} + A_{12} \cos(4\pi f_e t + \varphi_3 + \varphi_1) + A_{13} \cos(8\pi f_e t + \varphi_4 + \varphi_5)
\end{aligned} \tag{A.1}$$

— ε^4

$$\begin{aligned}
&\ddot{u}_4 + 2c\dot{u}_4 + \omega^2 u_4 = b_1 u_3 + b_2 u_2 + b_3 u_1 + b_4 u_0 - 2h u_0 u_3 - 2h u_1 u_2 \\
&\quad = b_2 A_7 \cos(2\pi f_e t + 2\varphi_0) + b_2 A_5 \cos(2\pi f_e t + 2\varphi_0 + \varphi_1) \\
&\quad + b_2 A_6 \cos(6\pi f_e t + 3\varphi_0 + \varphi_1 + \varphi_2) + b_4 A_0 \cos(2\pi f_e t + \varphi_0) \\
&\quad - 2h A_0 A_{11} \cos(2\pi f_e t + \varphi_0) - h A_0 A_{12} \cos(6\pi f_e t + \varphi_0 + \varphi_1 + \varphi_3) \\
&\quad - h A_0 A_{12} \cos(2\pi f_e t - \varphi_0 + \varphi_1 + \varphi_3) - h A_0 A_{13} \cos(10\pi f_e t + \varphi_0 + \varphi_4 + \varphi_5) \\
&\quad - h A_0 A_{13} \cos(6\pi f_e t - \varphi_0 + \varphi_4 + \varphi_5) - h A_1 A_7 \cos(6\pi f_e t + 4\varphi_0 + \varphi_1) \\
&\quad - h A_1 A_7 \cos(2\pi f_e t + \varphi_1) - h A_1 A_5 \cos(6\pi f_e t + 4\varphi_0 + 2\varphi_1) - h A_1 A_5 \cos(2\pi f_e t) \\
&\quad - h A_1 A_6 \cos(10\pi f_e t + 5\varphi_0 + 2\varphi_1 + \varphi_2) - h A_1 A_6 \cos(2\pi f_e t + \varphi_0 + \varphi_2) \\
&\quad - 2h A_2 A_7 \cos(2\pi f_e t + 2\varphi_0) - 2h A_2 A_5 \cos(2\pi f_e t + 2\varphi_0 + \varphi_1) \\
&\quad - 2h A_2 A_6 \cos(6\pi f_e t + 3\varphi_0 + \varphi_1 + \varphi_2) = A_{14} \cos(2\pi f_e t + \varphi_6) \\
&\quad + A_{15} \cos(6\pi f_e t + \varphi_7) + A_{16} \cos(10\pi f_e t + \varphi_8) \\
&b_4 = -A_0^{-1} \Big[b_2 A_7 \cos(\varphi_0) + b_2 A_5 \cos(\varphi_0 + \varphi_1) - 2h A_0 A_{11} \cos(0) \\
&\quad - h A_0 A_{12} \cos(-2\varphi_0 + \varphi_1 + \varphi_3) - h A_1 A_7 \cos(-\varphi_0 + \varphi_1) - h A_1 A_5 \cos(-\varphi_0) \\
&\quad - h A_1 A_6 \cos(\varphi_2) - 2h A_2 A_7 \cos(\varphi_0) - 2h A_2 A_5 \cos(\varphi_0 + \varphi_1) \Big] \\
&u_4 = A_{17} \cos(2\pi f_e t + \varphi_6 + \varphi_0) + A_{18} \cos(6\pi f_e t + \varphi_7 + \varphi_2) + A_{19} \cos(10\pi f_e t + \varphi_8 + \varphi_9)
\end{aligned} \tag{A.2}$$

References

1. Awrejcewicz J., 1996, *Deterministic Vibrations of Discrete Systems*, WNT, Warszawa, Poland [in Polish]
2. Belhaq M., Fahsi A., 2009, Hysteresis suppression for primary and subharmonic 3:1 resonances using fast excitation, *Nonlinear Dynamics*, **57**, 1/2, 275287
3. Bogusz W., Engel Z., Giergiel J., 1974, Oscillations and noise, *Printed Series of Course Lectures*, No. **347**, University of Mining and Metallurgy, Kraków, Poland, Wydawnictwa Geologiczne, Warszawa, Poland [in Polish]
4. Chajkin S.E., Lisovskij L.N., Solomonović A.E., 1939, On the dry friction forces, *Doklady Akademii Nauk SSSR*, **24**, 2, 134-138 [in Russian]

5. Chlebus E., Dybala B., 1999, Modelling and calculation of properties of sliding guide ways, *International Journal of Machine Tools and Manufacture*, **39**, 12, 1823-1839

6. Cunningham W.J., 1958, *Introduction to Nonlinear Analysis*, McGraw-Hill, New York

7. Dhupia J., Powalka B., Katz R., Ulsoy A.G., 2007, Dynamics of the arch-type reconfigurable machine tool, *International Journal of Machine Tools and Manufacture*, **47**, 2, 326-334

8. Fan K.C., Chen H.M., Kuo T.H., 2012, Prediction of machining accuracy degradation of machine tools, *Precision Engineering*, **36**, 2, 288-298

9. Fyrillas M.M., Szeri A.J., 1998, Control of ultra- and subharmonic resonances, *Journal of Nonlinear Science*, **8**, 2, 131-159

10. Grigorova S.R., Tolstoi D.M., 1966, On the resonance descending of friction force, *Doklady Akademii Nauk SSSR*, **167**, 3, 562-563 [in Russian]

11. Grudziński K., Konowalski K., Kostek R., 2000, Untersuchung normaler Schwingungen der gefgten Körper bei Führungssystemen von Maschinen, *Machine Tools, Automation and Robotics in Mechanical Engineering*, Praha, Section 1, 236-242, 20-22.6.2000

12. Grudziński K., Kostek R., 2007, An analysis of nonlinear normal contact microvibrations excited by a harmonic force, *Nonlinear Dynamics*, **50**, 4, 809-815

13. Gutowski P., 2003, Identyfikacja parametrów modeli dynamicznych układów nośnych obrabiarek, *Prace Naukowe Politechniki Szczecińskiej, Wydział Mechaniczny*, **574** [in Polish]

14. Hess D.P., Soom A., 1991a, Normal vibrations and friction under harmonic loads: Part I – Hertzian contacts, Part II – Rough planar contacts, *ASME Journal of Tribology*, **113**, 1, 80-86

15. Hess D.P., Soom A., 1991b, Normal vibrations and friction under harmonic loads: Part II – Rough planar contact, *ASME Journal of Tribology*, **113**, 1, 87-92

16. Hess D.P., Soom A., 1992, Normal and angular motions at rough planar contacts during sliding with friction, *Journal of Tribology*, **114**, 3, 567-578

17. Hess D.P., Wagh N.J., 1995, Evaluating surface roughness from contact vibrations, *Journal of Tribology*, **117**, 1, 60-64

18. Hunt K.H., Crossley F.R.E., 1975, Coefficient of restitution interpreted as damping in vibroimpact, *ASME Journal of Applied Mechanics*, **42**, 2, 440-445

19. Huo D., Cheng K., Wardle F., 2010, A holistic integrated dynamic design and modelling approach applied to the development of ultra-precision micro-milling machines, *International Journal of Machine Tools and Manufacture*, **50**, 4, 335-343

20. Kaminskaya V.V., Levina Z.M., Reshetov D.N., 1960, *Staninyi korpusnye detali metallorezhushchikh stankov*, Mashgiz, Moscow [in Russian]

21. Kligerman Y., 2003, Multiple solutions in dynamic contact problems with friction, *Proceedings of STLE/ASME International Tribology Conference*, Ponte Vedra Beach, FL, 1-8

22. Kostek R., 2002, Modelling and analysis of the natural frequency of an elastic body resting on rough surface, *Zeszyty Naukowe Katedry Mechaniki Stosowanej, Politechnika Śląska*, **18**, 213-218 [in Polish]

23. Kostek R., 2004, Investigations of the normal contact microvibrations and their influences on the reduction of the friction forces in a dynamical system, Ph.D. Thesis, Szczecin University of Technology, Szczecin, Poland [in Polish]

24. Levina Z.M., Reshetov D.N., 1971, *Contact Stiffness of Machines*, Mashinostroyenie, Moscow [in Russian]

25. Marchelek K., 1974, *Dynamika obrabiarek*, WNT Warszawa [in Polish]

26. Martins J.A.C., Oden J.T., Simões F.M.F., 1990, A study of static and kinetic friction, *International Journal of Engineering Science*, **28**, 1, 29-94

27. Moradi H., Bakhtiari-Nejad F., Movahhedy M.R., Ahmadian M.T., 2010, Nonlinear behaviour of the regenerative chatter in turning process with a worn tool: Forced oscillation and stability analysis, *Mechanism and Machine Theory*, **45**, 8, 1050-1066

28. Nayak P. R., 1972, Contact vibrations, *Journal of Sound and Vibration*, **22**, 3, 297-322

29. Nayfeh A.H., 1983, The response of single degree of freedom systems with quadratic and cubic non-linearities to a subharmonic excitation, *Journal of Sound and Vibration*, **89**, 4, 457-470

30. Nayfeh A.H., Mook D.T., 1995, *Nonlinear Oscillations*, Wiley, New York

31. Neugebauer R., Denkena B., Wegener K., 2007, Mechatronic systems for machine tools, *CIRP Annals – Manufacturing Technology*, **56**, 2, 657-686

32. Parlitz U., Lauterborn W., 1985, Superstructure in the bifurcation set of the Duffing equation $\ddot{x} + d\dot{x} + x + x^3 = f\cos(\omega t)$, *Physics Letters A*, **107**, 8, 351-355

33. Perret-Liaudet J., 1998, Superharmonic resonance of order two on a sphere-plane contact, *Comptes Rendus de l'Académie des Sciences – Series IIB*, **326**, 12, 787-792

34. Perret-Liaudet J., Rigad E., 2007, Superharmonic resonance of order 2 for an impacting Hertzian contact oscillator: Theory and experiments, *ASME Journal of Computational and Nonlinear Dynamics*, **2**, 2, 190-196

35. Rigaud E., Perret-Liaudet J., 2003, Experiments and numerical results on non-linear vibrations of an impacting Hertzian contact: Part 1: harmonic excitation, *Journal of Sound and Vibration*, **265**, 2, 289-307

36. Shi X., Polycarpou A.A., 2005, Measurement and modelling of normal contact stiffness and contact damping at the meso scale, *ASME Journal of Vibration and Acoustics*, **127**, 4, 52-60

37. Tang J., 2000, The MLP method for subharmonic and ultraharmonic resonance solutions of strongly nonlinear systems, *Applied Mathematics and Mechanics*, **21**, 10, 1153-1160

38. Thomas T. R., 1999, *Rough Surfaces*, Imperial College Press, UK

39. Thompson J.M.T., Stewart H.B., 2002, *Nonlinear Dynamics and Chaos*, Wiley, Chichester, UK

40. Tolstoi D.M., 1967, Significance of the normal degree of freedom and natural normal vibrations in contact friction, *Wear*, **10**, 3, 199-213

Analiza rezonansu kontaktowego głównego oraz rezonansów ultraharmonicznych – Część 1

Streszczenie

W artykule tym przedstawiono wyniki badań numerycznych oraz analitycznych drgań kontaktowych normalnych. Drgania te zostały wzbudzone przez siłę harmoniczną w układzie składającym się z dwóch ciał, które tworzą parę cierną. Głównym celem pracy było zbadanie zmian rezonansów kontaktowych pod wpływem wzrostu amplitudy wymuszenia. Oprócz rezonansu głównego zaobserwowano także rezonanse ultraharmoniczne, które są wzbudzane dla częstotliwości będących poniżej częstotliwości własnej układu. Amplituda rezonansów ultraharmonicznych staje się stopniowo większa wraz ze wzrostem amplitudy wymuszenia. Ponadto zaobserwowano asymetrię drgań kontaktowych, odrywanie się ciał od siebie, wiele atraktorów dla takiego samego wzbudzenia oraz zaginanie się pików rezonansowych. Wymienione zjawiska zaobserwowano dla nieliniowego układu o jednym stopniu swobody.

Manuscript received August 11, 2011; accepted for print November 11, 2012